TanDEM-X Performance Analysis.

Sigurd Huber, Marwan Younis, Gerhard Krieger
German Aerospace Center (DLR), Wessling, Germany

Abstract

TanDEM-X (**T**erraSAR-X **a**dd-o**n** for **D**igital **E**levation **M**easurement) [1] is a space borne X-band earth observation mission with the goal of generating a global Digital Elevation Model (DEM) with an unprecedented accuracy, corresponding to the HRTI-3 specifications. In the first part of the paper, the height performance model is presented. The analysis is extended to different terrain-types, showing a significant impact on the height accuracy. Based on a global terrain classification map, a first rough estimate of the global DEM performance is given. The second part concentrates on an analysis of the effect of the block adaptive quantiser (BAQ) in terrain with high dynamic range in backscatter power, like urban areas. Simulation results based on TerraSAR-X measurement data will be presented.

1 Introduction

The term performance has a wide spectrum of meanings. Here performance refers to the key quality parameter of any DEM, the height accuracy. Due to the nature of SAR imaging, the height accuracy is a statistical quantity and therefore all predictions have probabilistic character. The performance is influenced by various other parameters, like geometrical parameters or SAR system parameters. This offers the opportunity not only to estimate the performance of a given SAR system, but also to manipulate certain settings in order to improve the height accuracy.
Mandatory for any design is an understanding of the physical and technical aspects of radar imaging. The purpose of this paper is to give a brief outline of the performance model, which forms the basis for parameter selection and finally to estimate the global height accuracy within a so called Reference Scenario. The analysis is supplemented by an investigation of quantization effects in heterogeneous backscatter terrain. These quantization effects can degrade the height accuracy significantly and hence demand a careful selection of the BAQ settings.
The TanDEM-X DEM requirements are conform to the HRTI-3 specifications, listed in **Table 1**.

Requirement	**Spec.**	**HRTI-3**
absolute vertical accuracy (global)	$90\,\%$ linear error	$10\,\mathrm{m}$
relative vertical accuracy $1^\circ \times 1^\circ$ cell	$90\,\%$ linear point-to-point error	$2\,\mathrm{m}, \lvert\alpha\rvert \leq 20\,\%$ $4\,\mathrm{m}, \lvert\alpha\rvert > 20\,\%$

Table 1: HRTI-3 DEM specifications

The absolute vertical height inaccuracy shall not exceed $10\,\mathrm{m}$. Since the absolute height deviation is mostly contributed by low frequency errors, it can be compensated by proper calibration techniques. Therefore these error types are not considered here. Distortions which cannot be corrected are random errors, like thermal receiver noise. Here the height error limit is $2\,\mathrm{m}$ for terrain slopes α less than $20\,\%$ and $4\,\mathrm{m}$ for slopes greater than $20\,\%$.

2 Performance Model

The principle of SAR interferometry is to utilize the phase difference between two coregistered SAR images. After phase unwrapping and geocoding the phase difference is transformed into terrain height with respect to a reference Earth-model, here WGS84. A measure of the quality of an interferogram is the correlation coefficient or coherence [3]. Given the complex valued SAR images f_1 and f_2 the correlation coefficient is defined as

$$\gamma = \frac{\mathcal{E}\{f_1 f_2^*\}}{\sqrt{\mathcal{E}\{f_1 f_1^*\}\mathcal{E}\{f_2 f_2^*\}}} \quad . \tag{1}$$

Among error sources like ambiguous signal returns, coregistration errors or volume decorrelation, the major degradation of the coherence is caused by thermal receiver noise. In terms of signal to noise ratio (SNR), the coherence can be expressed as

$$\gamma_{SNR} = \frac{1}{\sqrt{\left(1 + SNR_1^{-1}\right)\left(1 + SNR_2^{-1}\right)}} \quad , \tag{2}$$

where the indices denote the two interferometric channels. Assuming uncorrelated errors, the total coherence can then be approximated by the product of all error contributions. Depending on the coherence γ and the number of independent looks n_L, the distribution of the interferometric phase errors $\Delta\phi$ is described by the probability density function

(pdf) [2]

$$p_{\Delta\phi}(\Delta\phi) = \frac{\Gamma(n_{\mathrm{L}}+0.5)(1-|\gamma|^2)^{n_{\mathrm{L}}}|\gamma|\cos\Delta\phi}{2\sqrt{\pi}\Gamma(n_{\mathrm{L}})(1-|\gamma|^2\cos^2\Delta\phi)^{n_{\mathrm{L}}+0.5}} + \frac{(1-|\gamma|^2)^{n_{\mathrm{L}}}}{2\pi}\,{}_2F_1(n_{\mathrm{L}},1;0.5;|\gamma|^2\cos^2\Delta\phi) \quad . \quad (3)$$

Here Γ denotes the gamma function and ${}_2F_1$ is the Gauss hypergeometric function. The $90\,\%$ point-to-point error is defined via the integral over the difference pdf of two phase errors in a $1^\circ \times 1^\circ$ cell, which corresponds approximately to a $100 \times 100\,\mathrm{km}^2$ square. Therefore, the joint pdf, which is given by the convolution of the single phase error pdfs, has to be evaluated:

$$\int_{-\Delta\phi_{90\%}}^{\Delta\phi_{90\%}} p_{\Delta\phi}(\Delta\phi) * p_{\Delta\phi}(\Delta\phi)\mathrm{d}\Delta\phi = 0.9 \quad . \quad (4)$$

The relative height error is then derived by scaling the interferometric phase error with the height of ambiguity:

$$\Delta h_{90\%} = h_{\mathrm{amb}}\frac{\Delta\phi_{90\%}}{2\pi} \quad . \quad (5)$$

A further improvement of the DEM accuracy can be achieved by combining overlapping data segments from successive TanDEM-X satellite passes. The redundant interferometric signals from overlapping beams can be used to partially compensate the performance decay at each swath border and to improve thereby the overall interferometric height accuracy. The resulting height error Δh after optimum combination is then given as

$$\Delta h = \left(\sum_{i=1}^{K_j}\Delta h_{90\%,i}^{-2}\right)^{-\frac{1}{2}} \quad . \quad (6)$$

K_j denotes the number of interferometric acquisitions at the jth pixel. Due to geometrical reasons, K_j is not the same for every pixel.
With this, the basis for a global performance estimate is formed.

2.1 Performance Reference Scenario

The purpose of the Reference Scenario is to demonstrate that a global DEM according to the HRTI-3 specifications is feasible.

scatterer type	height [m]	percentage [%]
soil & rock	-	13.4
grasses	-	18.3
short vegetation	2	30.6
shrubs	5	20.4
trees	20	17.0

Table 2: Global scatterer occurrence with representative vegetation heights

The key idea is to take into account different terrain types proportional to their occurrence. The terrain types are taken from a global land cover classification map. These land cover types are reduced to five different scattering classes (soil & rock, trees, grasses, shrubs and short vegetation) as seen in **Table 2**. In order to estimate volume decorrelation, a representative vegetation height is assigned to every scatterer type. The percentage numbers refer to the scatterers global occurrence.

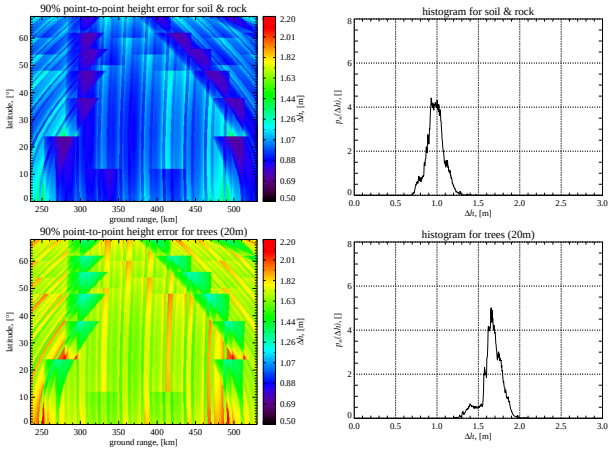

Figure 1: 90% height error after optimum combination (left column); histogram (right column)

Figure 1 shows exemplary the results for two scattering classes - soil & rock and trees. In the left column, the 90% point-to-point height error as function of the geographical latitude and ground range is depicted. Ground range is measured, starting at the intersection point of the earth surface with the position vector of the interferometer. On the right side, the corresponding histograms are plotted. As expected, the influence of volume decorrelation shifts the height errors towards higher values.

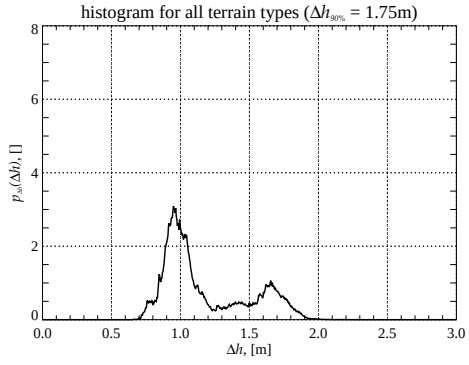

Figure 2: Global height error distribution

In **Figure 2** the global height error distribution is presented. The derived 90% height of $1.75\,\mathrm{m}$ is compliant to the HRTI-3 requirement.

3 Performance in heterogeneous Backscatter Terrain

Up to now, for the performance analysis, a homogeneous distribution of the backscatter was assumed. This is an assumption which holds for example for large vegetated areas like rain forest or for deserts. But in densely populated areas, a high dynamic range in backscatter can be expected. Especially man made structures like urban areas will reflect back more energy than natural scenes. Of special importance are land city transitions, where low and high scatterers are in close neighborhood.
Generally, a quantized signal is degraded by two error sources - granular noise and overload distortion or clipping errors. The effect considered here is called low scatterer suppression and is caused by inhomogeneous backscatter distributions. In the following the impact of quantization of signal returns from heterogeneous backscatter scenes on the height accuracy shall be analysed.

3.1 The Quantization Effect

The quantizer used in the TanDEM-X and TerraSAR-X satellite, respectively, is an 8 Bit Analog-to-Digital Converter (ADC) followed by a Block Adaptive Quantizer. The BAQ quantizes blocks of 128 samples of the input rawe data stream u separately for the inphase- and quadrature-channel (u_I and u_Q). Based on the signal statistics, BAQ specific parameters are calculated, which can vary from block to block. The compression levels are 8:2, 8:3, 8:4, 8:6 and BAQ8:8, the last corresponds to BAQ bypass.

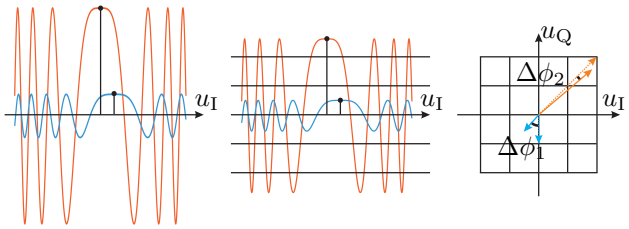

Figure 3: Quantization of SAR raw data

Figure 3 shows on the left hand side the inphase-channel u_I consisting of two chirp signals originating from two point sources in close vicinity. This signal is weighted in order to fit in a fixed amplitude interval and quantized by means of the ADC and the BAQ as indicated in the middle image. The weak signal will be quantized very roughly and therefore be distorted by more granular noise than the strong signal. What this means for the phase error is depicted on the right side. Here the corresponding vectors $u = [u_\mathrm{I}, u_\mathrm{Q}]^\top$ are shown. The phase error $\Delta\phi$ is the angle between the solid vector and the quantized dotted vector. In the worst case, the phase error is $45\,^\circ$. Those high phase errors are characteristic for the roughly quantized signals and therefore $\Delta\phi_1$ from the low signal is expected to be larger than $\Delta\phi_2$ in the most cases.
After focusing, in the SAR images both, the strong and the weak scatterers, are resolved. Consequently, regions with strong scatterers, which are quantized adequately will show low phase errors, while low backscatter regions are formidably more distorted. The amount of granular noise depends on the dynamic range of the backscatter.

3.2 Simulation Approach

By means of simulations, the effect shall be characterized and its dependence on the clipping is analysed.

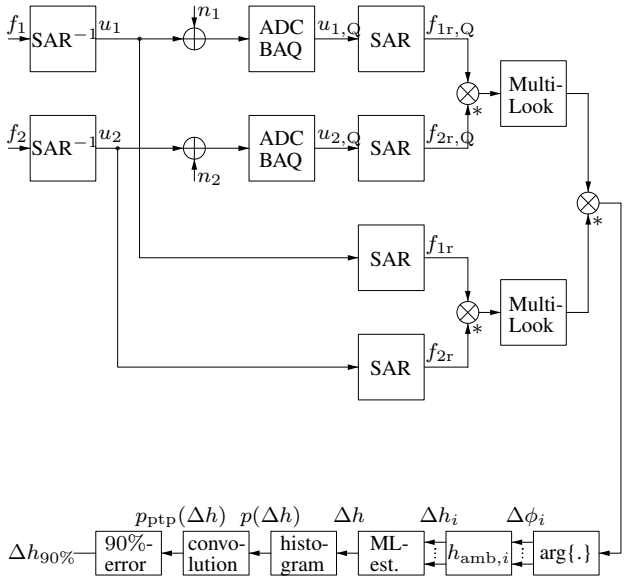

Figure 4: system model representing the interferometric chain with post processing

The simulation flow chart is illustrated in **Figure 4**. Starting with an interferometric image pair f_1 and f_2 the SAR raw data is generated by convolving the scene with the inverse focusing kernel. The raw data is superimposed by thermal receiver noise n_1 and n_2 and quantized. After focusing, the interferogram is formed from $f_{1\mathrm{r,Q}}$ and $f_{2\mathrm{r,Q}}$. Multilook processing reduces the speckle effect. The resulting interferometric phase is compared to the case where no thermal receiver noise and no quantization errors are present (lower path). The result is a phase error image $\Delta\phi_i$, where the index i accounts for multiple realizations. At this point the height error is simply calculated according to

$$\Delta h_i = h_{\mathrm{amb},i}\frac{\Delta\phi_i}{2\pi} \quad . \tag{7}$$

Since it is planned to image the earth surface twice with different baselines, the heights of ambiguities are assumed to be constantly $30\,\mathrm{m}$ and $40\,\mathrm{m}$, respectively. After optimum combination of the single height measurements, the histogram can be computed. The $90\,\%$ point-to-point height error $\Delta h_{90\,\%}$ is finally derived from the point-to-

point height error distribution $p_{\mathrm{ptp}}(\Delta h) = p(\Delta h) * p(\Delta h)$ (compare to (4)).

3.3 Simulation Results

In a first approach an artificial scene with a rectangular scatterer profile in azimuth direction was simulated. The backscatter step height $\Delta\sigma_0$ is $15\,\mathrm{dB}$, which can be regarded as typical mean dynamic range in urban areas.

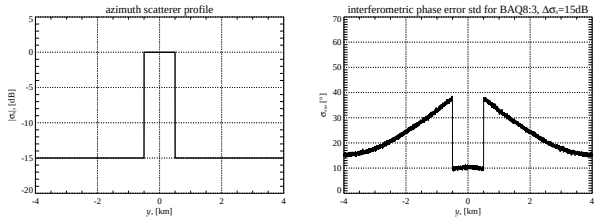

Figure 5: Azimuth scatterer profile (left) and standard deviation of the interferometric phase error (right)

Figure 5 shows the azimuth scatterer profile and the corresponding standard deviation of the interferometric phase error for a BAQ compression ratio of 8:3. The increase of the phase errors towards the region with high scatterer power between $\pm 500\,\mathrm{m}$ can be clearly observed. The extension of the zone with increased errors is proportional to the azimuth beam width, which is in the order of $4\,\mathrm{km}$ for an incidence angle of $30\,^\circ$. In range direction the errors are spread proportional to the transmitted pulse length.
The following simulations are based on TerraSAR-X measurement data over Cairo, Egypt. This scene offers a high dynamic range in backscatter power.

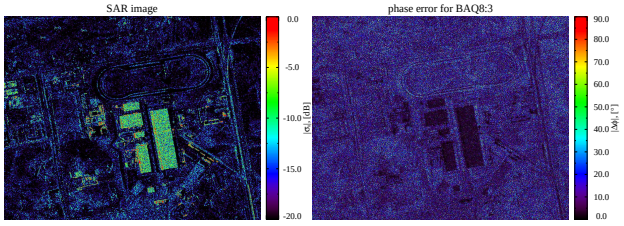

Figure 6: SAR image with high dynamic range (left) and corresponding interferometric phase error for BAQ8:3 (right)

To make the low scatterer suppression effect visible, a small area including some buildings was analysed. The left plot in **Figure 6** shows the SAR image with a mean backscatter dynamic in the order of 15 to $20\,\mathrm{dB}$. The corresponding phase error is depicted on the right side. As expected, the strong scatterers are less distorted than the low scatterer regions. It is important to note, that thermal receiver noise produces similar phase error distributions. Both error sources, the quantization errors and thermal noise, can be treated as additive. This is an approximation, since quantization is a nonlinear operation.

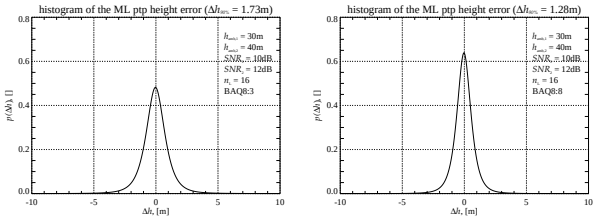

Figure 7: Histogram for the point-to-point height error after optimum combination of the two interferometric acquisitions for BAQ8:3 (left) and BAQ8:8 (right)

The histogram in **Figure 7** shows the distribution of the height errors for BAQ8:3 (left) in comparison to BAQ8:8. This simulation is based on a large part of the Cairo scene. Here a mean SNR of $10\,\mathrm{dB}$ and $12\,\mathrm{dB}$ for the two interferometric acquisitions is assumed. These are typical values observed in TerraSAR-X stripmap images. The 90% height error increases from $1.28\,\mathrm{m}$ to $1.73\,\mathrm{m}$.

4 Conclusion

On the basis of a Performance Reference Scenario the height performance for a global DEM was demonstrated. The analysis was supplemented by comprehensive simulations with real TerraSAR-X measurement data in order to demonstrate the impact of heterogeneous backscatter on the performance. Concerning future investigations, the Reference Scenario should be refined to that effect, that not only the global scatterer distribution is taken into account, but also terrain slopes.

5 Acknowledgement

The TanDEM-X project is partly funded by the German Federal Ministry of Economics and Technology (Förderkennzeichen 50 EE 0601).

References

[1] Gerhard Krieger, Alberto Moreira, David Hounam, Marian Werner, Sebastian Riegger, and Eckard Settelmeyer. A Tandem TerraSAR-X Configuration for Single-Pass SAR Interferometry. *Proceedings of the International Conference on Radar Systems*, 2004.

[2] Jong-Sen Lee, Karl W. Hoppel, Stephen A. Mango, and Allen R. Miller. Intensity and Phase Satistics of Multilook Polarimetric and Interferometric SAR Imagery. *IEEE Transactions on Geoscience and Remote Sensing*, 32(5):1017–1028, September 1994.

[3] Howard A. Zebker and John Villasenor. Decorrelation in Interferometric Radar Echos. *IEEE Transactions on Geoscience and Remote Sensing*, 30(5):950–959, September 1992.